Heterobimetallic-mediated dinitrogen functionalization: N–C bond formation at rhenium-group 9 diazenido complexes

Erik T. Ouellette,[†,§] Julian S. Magdalenski,[†] Robert G. Bergman,[†] John Arnold[†,§,*]

[†]*Department of Chemistry, University of California, Berkeley, California 94720, USA*
[§]*Chemical Sciences Division, Lawrence Berkeley National Laboratory, Berkeley, California 94720, USA*

*Email: arnold@berkeley.edu

Abstract

We report the synthesis and characterization of rhenium-group 9 heterobimetallic diazenido species (η^5-Cp)Re(μ-BDI)(μ-N_2)M(COD) (**1-M**, M = Ir or Rh, Cp = cyclopentadienide, BDI = N,N′-bis(2,6-diisopropylphenyl)-3,5-dimethyl-β-diketiminate, COD = 1,5-cyclooctadiene), formed from salt elimination reactions between Na[(η^5-Cp)Re(BDI)] and [MCl(η^4-COD)]$_2$. Additionally, we find that these same reagents react under an argon atmosphere to instead produce bridging hydride complexes (BDI)Re(μ-η^5:η^1-C_5H_4)(μ-H)M(COD) (**2-M**), which undergo rearrangements upon protonation to form the alternative bridging hydrides [(η^5-Cp)Re(μ-BDI)(μ-H)M(COD)][(B(*m*-$C_6H_3(CF_3)_2)_4$] (**3-M**). Further, we demonstrate the first example of N–C bond formation at a heterobimetallic dinitrogen complex through reactions of **1-M** and methyl triflate, which produces the alkylated species [(η^5-Cp)Re(μ-N(Me)N)(μ-BDI)M(COD)][OTf] (**4-M**, OTf = trifluoromethanesulfonate). A combination of spectroscopic studies, X-ray structural analysis, and computational investigations are discussed as an aid to understanding the modes of dinitrogen activation within these unique heterobimetallic complexes.

Introduction

Examination of the introductory paragraphs of review articles pertaining to transition metal-mediated dinitrogen activation reveals several essential and often-repeated points: (1) dinitrogen (N_2), while enormously abundant in Earth's atmosphere, is extremely unreactive due to its large bond dissociation energy and sizable HOMO-LUMO gap; (2) the major industrially relevant method for N_2 fixation, the Haber-Bosch process, requires enormous amounts of energy and utilizes harsh conditions to convert N_2 to ammonia (NH_3); and (3) development of new molecular systems that can effectively activate or functionalize dinitrogen are crucial to improving our understanding of biological and synthetic N_2 fixation.[1–6] While remarkable achievements have been made within the field of N_2 fixation and functionalization, the overwhelming majority of these efforts have focused on N–H bond formation for both the stoichiometric and catalytic conversion of N_2 to NH_3 (or N_2H_4).[1–4,6] Although ammonia is undoubtedly an essential nitrogen feedstock molecule, synthetic methods to directly convert N_2 to more complex N-containing molecules, whether through N–C, N–Si, or even N–B bond formation, are much less refined than those towards NH_3 formation.[6–8]

The manner in which N_2 coordinates to a metal center, and its resulting reactivity patterns, can be influenced by the number of metal centers present, as well as covalent and noncovalent interactions in the secondary sphere. Monometallic species are effectively limited to end-on coordination of N_2, in which functionalization can occur either exclusively at the more nucleophilic distal nitrogen or in an alternating fashion at both N atoms.[9,10] In contrast, bimetallic species exhibit widely varied reactivity patterns, due to

the fact that electron density is often delocalized across the entire dinitrogen fragment; in addition, the N_2 ligand can be bound in either an end-on/end-on, side-on/side-on, or (the rare) end-on/side-on fashion (Scheme 1).[6,7,10] Bimetallic complexes are also capable of a "dissociative" activation strategy in which cleavage of N_2 to form two terminal nitrides occurs prior to N functionalization.[6,11,12] Recently, models have been developed to predict the tendency of metal complexes to form terminal monometallic versus bridging bimetallic dinitrogen complexes,[13] which in turn should aid the design of species with desired reactivity patterns. Finally, transition metal-mediated N_2 functionalization can also be facilitated through the use of noncovalent or hydrogen bonding, coordination of Lewis acids (LAs), or other secondary sphere interactions (similar to those in nitrogenase active sites) to enhance dinitrogen activation and reactivity.[14–19] For example, Szymczak and coworkers found that coordination of LAs to the distal nitrogen of iron dinitrogen complexes causes a "push-pull" type activation[20] of the dinitrogen fragment that primes these complexes for protonation at the distal N atom and disfavors undesired protonation at the Fe center.[18]

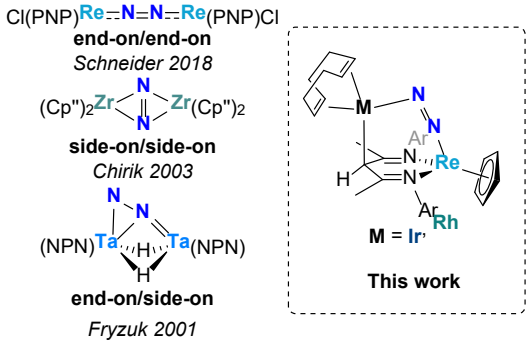

Scheme 1. Select examples of typical bimetallic transition-metal dinitrogen binding modes (left),[11,21,22] compared to the reported work.

Despite the array of design strategies for both mono- and bimetallic N_2 fixation, there are relatively few structurally characterized, molecular, heterobimetallic dinitrogen complexes in which both transition metal centers interact with an activated dinitrogen fragment.[23,24,33–36,25–32] Furthermore, to our knowledge, to date there are no reported examples of N–C bond formation at a heterobimetallic dinitrogen complex. As such, we reasoned that the exploration of heterobimetallic dinitrogen complexes that either display non-traditional dinitrogen coordination geometries or that enforce a "push-pull" activation effect between metal centers might increase the likelihood of N–C bond formation.

Our group has developed a highly-reducing rhenium(I) metalate, Na[Re(η^5-Cp)(BDI)] (Cp = cyclopentadienide, BDI = N,N′-bis(2,6-diisopropylphenyl)-3,5-dimethyl-β-diketiminate), capable of reversibly binding dinitrogen in solution at low temperatures, with the Na^+ counterion playing a crucial role in the binding and activation process.[23,37] Although there is some precedent for dinitrogen functionalization by rhenium complexes, both in monometallic complexes[38,39] and via the splitting of dinitrogen by homobimetallic species,[11,40–43] we were interested in the unexplored frontier of heterobimetallic dinitrogen functionalization. Through salt elimination reactions between the above-mentioned Na[Re(η^5-Cp)(BDI)] with either iridium(I) or rhodium(I) reagents, we report the synthesis, characterization, and initial N–C bond formation reactivity of Re-group 9 heterobimetallic dinitrogen species. In addition, we explore the chemistry of a set of Re-group 9 bridging hydride complexes formed from the divergent reactivity of identical starting materials reacted under an argon atmosphere.

Results and Discussion

Synthesis of Rhenium-Group 9 Diazenido Complexes

In designing heterobimetallic complexes using Na[Re(η^5-Cp)(BDI)] as a starting material, the highly reducing nature of the rhenium(I) metalate necessitated that we employ low-valent transition metal partners resistant to reduction.[44] Given this requirement, we considered the robust monovalent group 9 dimers [MCl(η^4-COD)]$_2$ (M = Ir, Rh, COD = 1,5-cyclooctadiene) as a suitable match, especially given that the presence of a chloride ligand would allow for salt elimination reactivity with our metalate. We conducted reactions in a nitrogen-filled glovebox and at low temperatures (–78 °C) to favor N_2 binding. Under these conditions, reactions of Na[Re(η^5-Cp)(BDI)] and [MCl(η^4-COD)]$_2$ led to isolation of the bimetallic complexes **1-M** (Scheme 2, top), in which bound dinitrogen had been trapped between the rhenium and group 9 metal centers. Progression of the reactions was not readily apparent by their appearance, as the reaction solution maintained a deep maroon color throughout. However, upon removal of THF the reaction residue contained a noticeable greenish-brown component to it. After extraction with Et_2O, diazenido complexes **1-M** crystallized from solution as dark, forest green crystals in moderate yields.

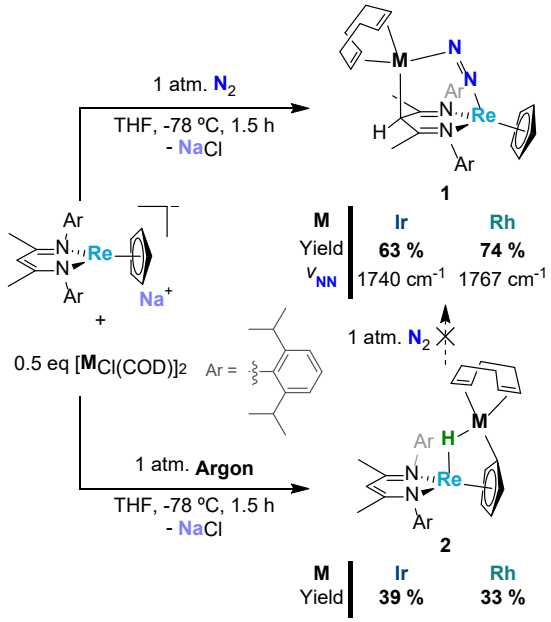

Scheme 2. Syntheses of diazenido complexes **1-M** and bridging hydride complexes **2-M** (M = Ir, Rh), depending on reaction atmosphere.

X-ray crystallographic determination of the structures of **1-M** supported incorporation of dinitrogen as a bridged ligand between rhenium and iridium/rhodium metal centers (Figure 1). Interestingly, instead of a group 9–COD complex bound only to the terminal diazenido nitrogen, the Ir(I) or Rh(I) metal centers also interact with the backbone of the BDI ligand, allowing them to retain their favorable square planar, 16 e$^-$ geometry. NMR spectra confirmed connectivity between rhodium and the BDI backbone carbon (C8), as we observed both single bond coupling between ^{103}Rh (I = ½, 100%) and C8 in the ^{13}C NMR spectra ($^1J_{Rh–C}$ = 14.6 Hz, Figure S4), as well as two-bond coupling to the proton attached to C8 in the ^{1}H NMR spectra ($^2J_{Rh–H}$ = 2.0 Hz, Figure S3). Thus, complexes **1-M** are examples of unusual bridging dinitrogen species in which the metals are also tethered together via a bridging BDI ligand. The coordination geometry of dinitrogen in complexes **1-M** should not be considered as a standard end-on/end-on mode, as **1-M** demonstrate much shorter contacts to rhenium [Re–N3: 1.836 Å] than the group 9 metal [M–N4: 2.095(7) for **1-Ir**, 2.124(5) for **1-Rh**] and the Re–N3–N4 angles are nearly linear [171.0(7)° and 174.5(5)° for **1-Ir**

and **1-Rh**, respectively] while the M–N4–N3 angles are bent [116.5(6)° and 112.2(4)°] (see Table S3 for detailed bond metrics). This geometry is unique compared to other reported transition metal dinitrogen species,[45] and we are unaware of any bimetallic complexes that feature a similar non-linear, end-on/end-on coordination.[46]

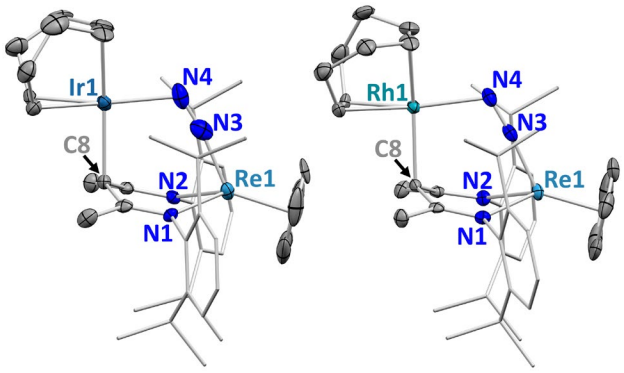

Figure 1. X-ray crystal structures of **1-Ir** (left) and **1-Rh** (right) shown with 50% probability ellipsoids. The BDI aryl groups are shown in wireframe, and hydrogen atoms are omitted for clarity.

The dinitrogen moiety in these molecules is significantly reduced, displaying N–N infrared (IR) stretching frequencies of 1740 and 1767 cm^{-1}, compared to 2359 cm^{-1} for free N_2,[47] with the stretch in **1-Ir** slightly lower in energy (more reduced) relative to **1-Rh** (Figures S24 and S25). Despite spectroscopic evidence for activated dinitrogen, the N–N distances in the solid-state [1.10(1) Å for **1-Ir** and 1.148(7) Å for **1-Rh**] were minimally elongated relative to free N_2 (1.098 Å).[48] We recently reported rhenium-silane and -silylene diazenido complexes [Re(N=NSiMe$_3$)(η^5-Cp)(BDI)[23] and Re(N=NSi[PhC(N^{t}Bu)$_2$])(η^5-Cp)(BDI)[49]] synthesized from the same Re(I) metalate starting material; compared to these species, the bimetallic dinitrogen species **1-M** display some distinct differences. The Si-functionalized diazenidos have slightly longer N–N bond distances (1.19–1.25 Å) and lower N–N bond stretching vibrations (1617–1682 cm^{-1}) than in **1-M**. They also have more highly bent Re–N3–N4 angles (159.6–168.9°), but also wider N3–N4–Si angles (127.5–137.2°) to go along with shorter Re–N3 distances (by ~0.05 Å) and much shorter N4–Si distances (by ~0.35 Å compared to N4–M distances). Many of these differences are likely due to the nature of the bridging BDI ligand in **1-M**, which enforces a more strongly bent (or side-on) coordination of the Ir/Rh atom to the distal nitrogen relative to those in the solely terminally-bound silicon analogues.

To probe the importance of Ir/Rh metal centers in activating dinitrogen in **1-M** via a push-pull type mechanism, we attempted to investigate the bonding in the "M–N–N–M" fragment. First, we tried synthesizing analogues to **1-M** that featured either more donating or accepting ligands than COD on the Ir/Rh center. Our expectation was that observing changes in the N–N stretching frequency of the heterobimetallic diazenido upon substitution of the COD ligand would provide valuable insight into whether the Ir/Rh center is aiding activation of N_2 either through a "push" or "pull" type effect. However, we were surprised to find that similar reactions employing [Rh(CO)$_2$Cl]$_2$ or RhCl(PPh$_3$)$_3$ instead of [Rh(COD)Cl]$_2$ were unsuccessful, leading either to formation of significant quantities of Re(η^5-Cp)(BDI) or intractable mixtures. Attempts to substitute COD directly from **1-M** using large equivalents of PPh_3 were similarly futile. It appears that the ligand characteristics of COD are ideally suited for the formation of **1-M**, which unfortunately precluded this approach to our goal of probing the bonding situation.

Turning to computational methods allowed some insight into the relevant bonding interactions in **1-M** (see SI for computational details). Analysis of the molecular orbitals of **1-M** using density functional theory revealed significant interactions between rhenium and the dinitrogen ligand, whereas the Ir/Rh interactions with dinitrogen were significantly less involved (Figure 2). We observe both σ- and π-type interactions between Re and N3, leading to a Wiberg Bond Index (WBI) for this bond of 1.41 (**1-Ir**) or 1.36

(**1-Rh**), consistent with moderate backbonding between N_2 and rhenium. Conversely, the bonding between N4 and Ir/Rh is only of σ-symmetry, with a WBI of just 0.54 (**1-Ir**) or 0.50 (**1-Rh**). Interestingly, the symmetry of the M–N4 bonding orbital is such that it arises from interaction of an N_2 π* orbital with Ir/Rh. We also see interaction between filled Re d-orbitals and this same N_2 π* orbital in the HOMO; as such, it is reasonable to presume there is a push-pull type interaction in **1-M**, in which electron density originating from rhenium is pushed through the N_2 ligand and pulled towards iridium/rhodium.

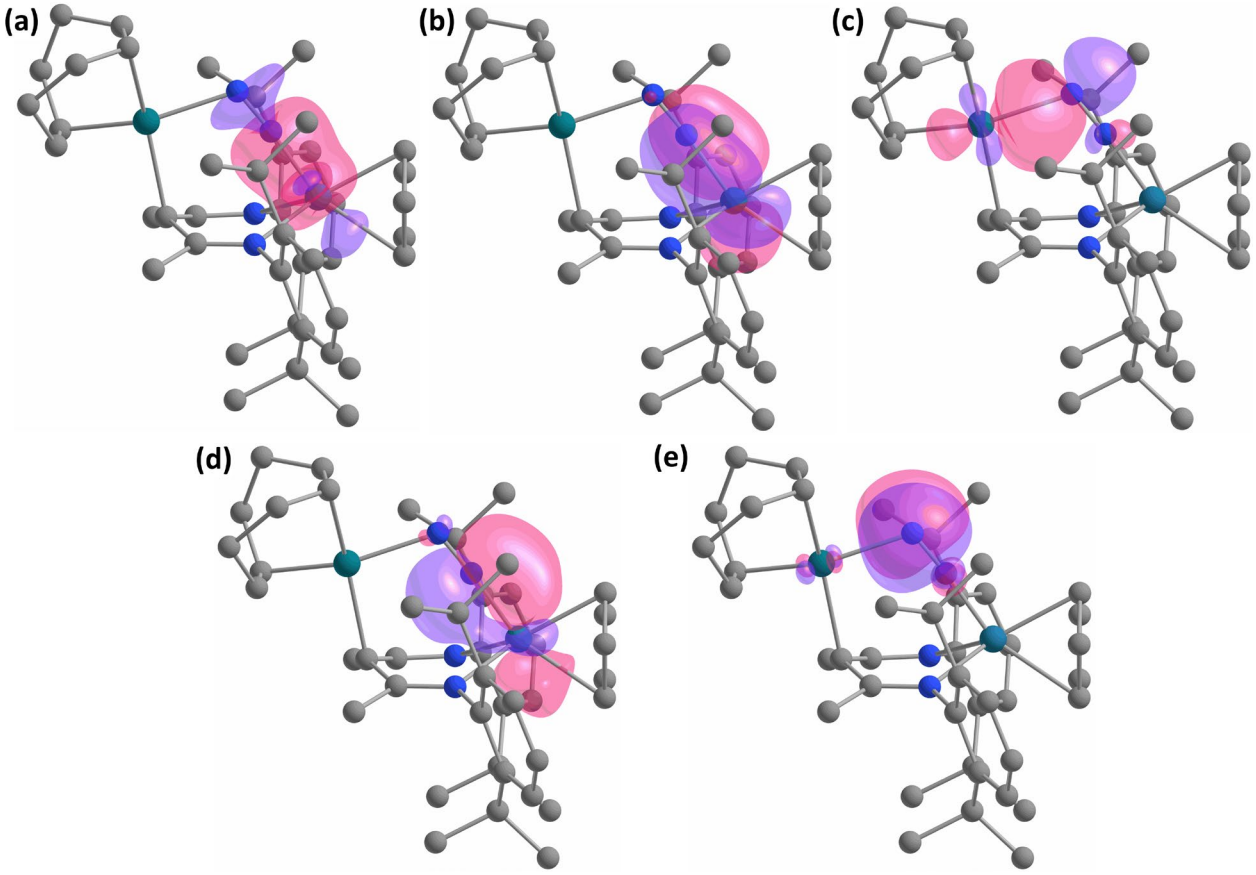

Figure 2. Renderings of select calculated molecular orbitals of **1-Rh**, including: (a) a Re–N σ-bonding orbital (HOMO-25), (b) a Re–N π-bonding orbital (HOMO-17), (c) the Rh–N bonding orbital (HOMO-18), (d) the HOMO, and (e) the LUMO (isovalue = 0.02).

Ultimately, we hypothesized that heterobimetallic complexes **1-M** may prime the dinitrogen fragment for further reactivity (see below), whether towards N–C bond formation or otherwise, due to the tethered nature of the Ir/Rh and Re centers, the steric accessibility of one face of the N–N fragment, and the ability of **1-M** to participate in push-pull type activation of the N–N bond.

Synthesis and Reactivity of Rhenium-Group 9 Bridging Hydride Complexes

While optimizing reaction conditions for syntheses of **1-M**, we noticed several peaks in the ^{1}H NMR spectra of crude reaction mixtures, particularly upfield resonances around -25 to -35 ppm, that hinted at the formation of minor products. Anticipating that an additional product might be formed without incorporation of dinitrogen, we attempted salt metathesis reactions in the absence of dinitrogen under argon. Under these conditions, reactions between Na[Re(η^5-Cp)(BDI)] and [MCl(η^4-COD)]$_2$ (M = Ir, Rh) led to isolation of dark red crystals of **2-M** (Scheme 2, bottom). A salient feature in the subsequent ^{1}H NMR

spectra of **2-M** was the presence of upfield resonances integrating to one proton located at –26.24 (for **2-Ir**) and –34.21 (for **2-Rh**) ppm, indicative of a rhenium hydride (Figures S5 and S7).[23,49,50] We had previously isolated rhenium-hydrides from salt elimination reactions of Na[Re(η^5-Cp)(BDI)] with silane and silylene halides, with hydride formation resulting from Si–C bond formation at a Cp carbon accompanied by migration of the displaced Cp hydrogen to rhenium.[23,49] The ^{1}H NMR spectra of **2-M** displayed two singlets integrating to two protons attributable to a C_5H_4X fragment (as opposed to a five proton singlet for a standard Cp ligand, C_5H_5), which supported our suspicion that a similar Cp substitution had occurred here with the "M(COD)" unit to form an M–C bond, in turn leading to formation of the observed rhenium-hydride peak. Additionally, however, the hydride peak in **2-Rh** presented as a doublet with J = 19.0 Hz, leading us to suspect a rhenium-hydride was also coupling to ^{103}Rh, perhaps due to a bridging hydride geometry.

Solid-state structures of **2-M** confirmed our spectroscopic assignments of an unusual bridging hydride geometry (Figure 3, Table S4). The Ir/Rh atoms had indeed substituted at a Cp carbon (C5), and the resulting hydride could be found bound between the two metal centers, which are separated by 2.7757(6) (for **2-Ir**) and 2.8987(6) (for **2-Rh**) Å. Unsurprisingly, the 16-electron Ir(I)/Rh(I) metal centers retain a square-planar geometry.

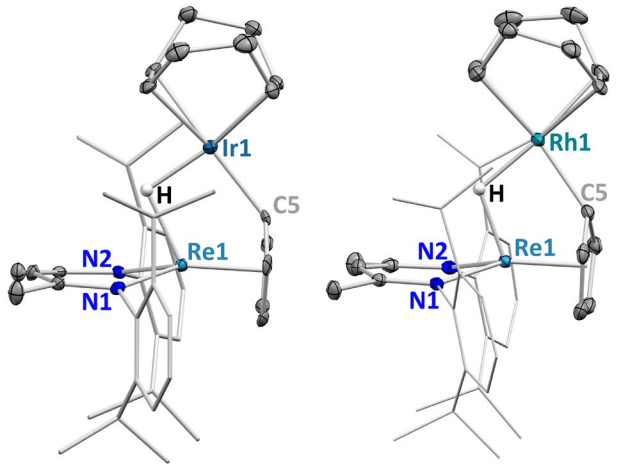

Figure 3. X-ray crystal structures of **2-Ir** (left) and **2-Rh** (right) shown with 50% probability ellipsoids. The BDI aryl groups are shown in wireframe, and hydrogen atoms (except for bridging hydrides) are omitted for clarity.

The divergent syntheses of **1-M** versus **2-M** depending on reaction conditions expands the synthetic potential of the Re(I) metalate starting material,[37] and left us with an interesting prospect for further investigating the dinitrogen binding ability of Re-group 9 bimetallic species. We were curious if it were possible to abstract the hydride in **2-M** under an N_2 atmosphere, and if so, whether abstraction might enforce either a direct M–M interaction or, alternatively, lead to reincorporation of dinitrogen to form a diazenido species analogous to **1-M**. Unfortunately, addition of $B(C_6F_5)_3$, a common hydride abstraction agent, to **2-M** led to intractable mixtures, and we moved instead to trying to protonate **2-M**, with the expectation that protonation of the hydride could lead to the loss of dihydrogen. Protonation of **2-M** with Brookhart's acid[51] led to deposition of a waxy red residue on the vial walls of the reaction mixture. Crystallization of this residue from an Et_2O/pentane mixture led to isolation of dark red crystals of a new product, **3-M** (Scheme 3). Characteristic shifts in the ^{1}H NMR of **3-M** (–40.10 ppm for **3-Ir**, –40.43 ppm for **3-Rh**), albeit even

further upfield than analogous shifts in **2-M**, were indicative of another metal hydride species. And again, the hydride shift in **3-Rh** displayed ^{103}Rh–H coupling ($^{1}J_{Rh-H}$ = 13.4 Hz).

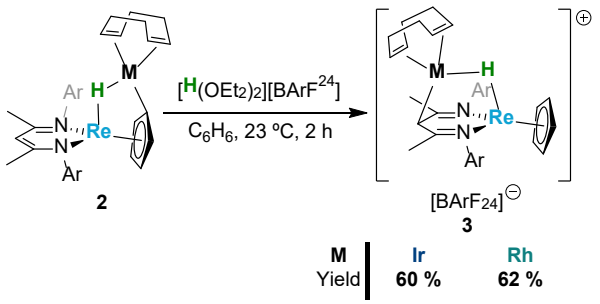

Scheme 3. Syntheses of cationic bridging hydride complexes **3-M** (M = Ir, Rh).

Solid-state structures of **3-M** supported the assumed connectivity in this new product, although difficulties in obtaining crystals of **3-M** of suitable size and quality led to non-ideal crystallographic data. As a result, despite numerous crystallization efforts, we were unable to locate bridging hydrogen atoms in the difference maps of these presumed bridging hydride species (Figure 4, Table S5). Protonation of **2-M** led to migration of the group 9 metal center, from its initial position bound to a Cp carbon, to the opposite side of the (η^5-Cp)Re(BDI) scaffold, now bound to the backbone carbon of the BDI ligand in a manner reminiscent to that in **1-M**. Staying in theme, the group 9 metal centers cling to their preferred square planar geometry in **3-M**. Notably, the distance between metal centers in **3-M** is significantly greater than in **2-M**, by ~0.2 Å, despite both being bridging hydride complexes of the same metals. Additionally, the Re–Cp(centroid) distances are lengthened by ~0.03 Å in **3-M**.

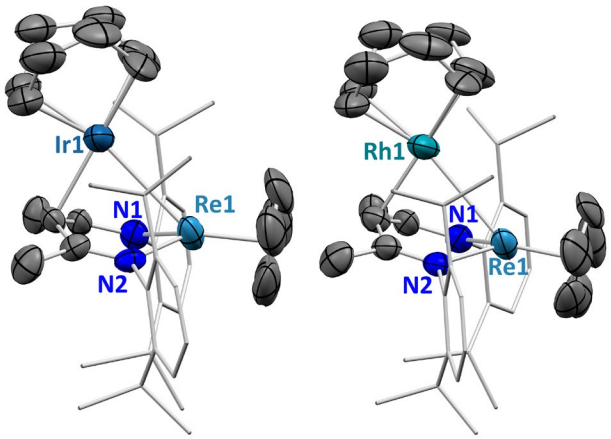

Figure 4. X-ray crystal structures of **3-Ir** (left) and **3-Rh** (right) shown with 50% probability ellipsoids. The BDI aryl groups are shown in wireframe, and hydrogen atoms and the counteranion are omitted for clarity. The bridging hydrides could not be located in the difference maps.

We were curious whether protonation occurred at a Cp carbon or at a metal center to replace the initial hydride in **2-M**. To probe this, we employed a deuterated analog of Brookhart's acid, [D(OEt$_2$)$_2$][(B(*m*-C$_6$H$_3$(CF$_3$)$_2$)$_4$], and carried out the analogous deuteration reaction of **2-Ir**. Subsequent NMR analysis of the resulting ^{2}H labeled product, **3-Ir-D**, revealed that protonation occurs at a Cp carbon: the Cp resonance in the ^{1}H spectrum only integrated to four protons and showed fine structure due to ^{1}H-^{2}H coupling, the ^{2}H spectrum contained a peak at 9.82 ppm (where we would expect to find a Cp proton

shift), and the ^{13}C spectrum displayed three peaks for the Cp carbons (as expected for a C_5H_4D unit, whereas C_5H_5 should display as a single shift) (Scheme S1, Figures S12-S14). In other words, the hydride that bridges between Re and Ir/Rh is not affected by the protonation reaction; protonation occurs solely at the Cp carbon and causes a geometric rearrangement of the Ir/Rh(COD) fragment. While we were unable to observe any direct metal-metal interactions during these hydride studies, they were useful in confirming that spontaneous dinitrogen incorporation into the rhenium-group 9 scaffold does not occur. Despite many manipulations of **2-M** and **3-M** under a dinitrogen atmosphere, we never observed evidence of dinitrogen binding to either the Re or Ir/Rh coordination spheres. As such, we believe that dinitrogen incorporation to form **1-M** likely occurs prior to addition of Ir/Rh, and these group 9 metal centers only aid in maximizing activation of N_2 rather than being integral to the original binding step.

N–C Bond Formation with Rhenium-Group 9 Diazenido Complexes

Given the lack of reported N–C bond formation reactions by heterobimetallic dinitrogen complexes, we were curious to know whether diazenido species **1-M** might be reactive towards alkylating agents. As such, we added MeOTf (OTf^- = trifluoromethanesulfonate, "triflate") to solutions of **1-M** in C_6D_6, and observed precipitation of light orange solids from the dark green/brown reaction mixture. While ^1H NMR spectra suggested substantial formation of Re(Me)(η^5-Cp)(BDI), which remained soluble in C_6D_6, the precipitates were isolated and a crude proton spectrum taken in THF-d_8 suggested formation of the desired methylated product. Optimization of the reaction conditions, including starting the reaction at low temperatures in toluene and employing strictly one equivalent of methyl triflate, subsequently allowed us to isolate the new methylated complexes, **4-M** (Scheme 3). While we could obtain microcrystalline **4-Ir** from solutions of THF, compound **4-Rh** initially cocrystallized with an unidentified minor product. Through subsequent recrystallizations from CH_2Cl_2/hexane mixtures, we were able to isolate exclusively **4-Rh**, although this resulted in a lower isolated yield overall. The ^1H NMR spectra of **4-M** showed clear singlet resonances (δ = 3.73 ppm for **4-Ir** in THF-d_8, 3.40 ppm for **4-Rh** in $CDCl_3$) that integrated to three protons, which were indicative of the presence of a new methyl group.

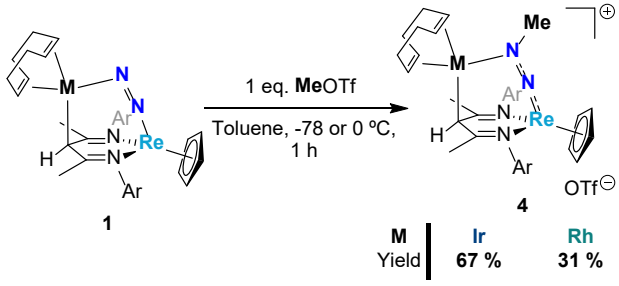

Scheme 4. Syntheses of methylated complexes **4-M** (M = Ir, Rh).

Solid-state structures of **4-M** confirmed the presence of a methyl group bound to a nitrogen proximal to the group 9 metal center (Figures 5 and S39, Table S6). The methylated cationic complexes were accompanied by an outer-sphere triflate counterion, and two of these ion pairs could be found in the asymmetric unit. The newly formed N–C bonds possessed lengths ranging from 1.44(3) to 1.48(4) Å. Furthermore, methylation of the diazenido complexes led to marked increases in N3–N4 bond lengths in **4-M**, which averaged 1.26 Å (as compared to an average of 1.12 Å in **1-M**). In line with further activation of the dinitrogen moeity, we observed stretching frequencies in the FTIR spectrum at 1565 cm^{-1} (for **4-Ir**) and 1568 cm^{-1} (**4-Rh**) that can tentatively be assigned to the NN bond (Figures S30 and S31). Computational analysis corroborated distinct changes in the bonding throughout the dinitrogen fragment in **4-M**. The calculated WBI values for the N–N bond decreased from 1.98 (**1-Ir**) or 2.04 (**1-Rh**) in the original

diazenidos to 1.37 (**4-Ir**) or 1.46 (**4-Rh**), consistent with both the experimental and calculated (see Table S8) increase in N–N bond distance upon functionalization with a methyl group. Despite methylation, the Re–N3–N4 bond angle remained fairly unchanged from the starting material, still at a near-linear 173-175°, while bent M–N4–N3 (M = Ir, Rh) angles of 108-111° were only slightly more acute than in **1-M**. However, the Re–N3 bond was ~0.11 Å shorter in **4-M** than in **1-M**, a significant decrease likely due to a strengthened bonding interaction between Re and N3. Calculations suggested precisely that, as the calculated WBI values for the Re–N3 bond increased to 1.98 (**4-Ir**) and 2.04 (**4-Rh**) compared to 1.36-1.41 in **1-M**. Additionally, an NBO analysis found both a σ-type and two π-type interactions between rhenium and N3 (Table S7), suggesting increased π-bonding between the two atoms than in **1-M**.

In contrast to **1-M**, there are two reported diazenido species comparable to **4-M**. Both (η^5-Cp)$(CO)_2$Mo(μ-$NNC_6H_4CH_3$)Re$(CO)_2(\eta^5$-Cp) [52] and (η^5-Cp)$(CO)_2$W(μ-$NNCH_3$)Cr$(CO)_5$ [53] have been reported, with the Mo/W metal centers bound end-on to a diazenido fragment which bonds through the opposite nitrogen to a carbon and Cr/Re metal center; these complexes were synthesized in a much different fashion, as they resulted from addition of the Lewis acids (η^5-Cp)Re$(CO)_2$(THF) or Cr$(CO)_5$ to the existing diazenidos (η^5-Cp)$(CO)_2$M(NNR) (M = Mo, W / R = $C_6H_4CH_3$, CH_3). As such, these examples do not represent any N–C bond formation reactivity.

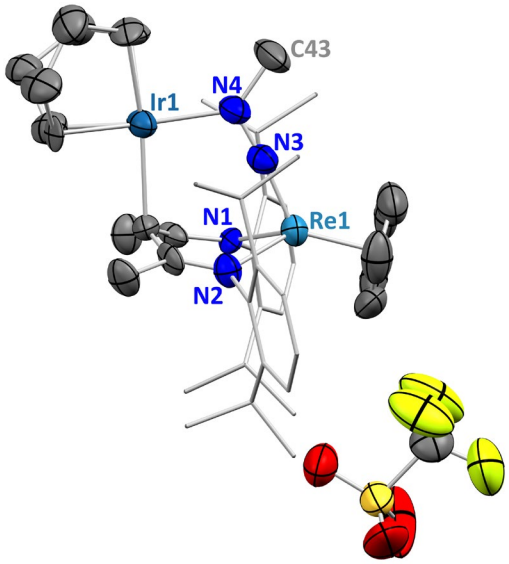

Figure 5. X-ray crystal structure of **4-Ir** shown with 50% probability ellipsoids. The BDI aryl groups are shown in wireframe, and hydrogen atoms are omitted for clarity.

The formation of an N–C bond with heterobimetallic dinitrogen complexes **1-M** is notable, especially considering these complexes were inert towards silylation and underwent alternative transformations with other alkyl and proton sources. Adding methyl iodide to **1-M** instead led to the formation of primarily Re(I)(η^5-Cp)(BDI),[54] and while [Me_3O][BF_4] led to partial conversion to form a methylated species similar to **4-M**, we observed a larger degree of conversion to Re(Me)(η^5-Cp)(BDI) in the product mixture than when using MeOTf. Protonation of **1-M** was similarly unsuccessful, as we primarily observed formation of previously reported Re(H)(η^5-Cp)(BDI), due to the high propensity of this rhenium system to form rhenium hydride species. We also assumed that silylation of **1-M** would proceed similarly to, or even more readily than, methylation. However, **1-M** was inert towards both Me_3SiCl and Me_3SiOTf, even at elevated temperatures. It is surprising that **1-M** is reactive towards methylation but not

silylation, especially considering there are significantly more examples by transition metal-dintrogen complexes of N–Si bond formation (both catalytic and stoichiometric), than of N–C bond formation.[6]

To determine whether our rhenium system is capable of diazenido methylation on its own (without heterobimetallic contributions from iridium/rhodium), we ran two control reactions: (1) low-temperature reactions between Na[Re(η^5-Cp)(BDI)] (which reversibly binds dinitrogen and may be considered as partially "Na[Re(N_2)(η^5-Cp)(BDI)]" in solution) and MeOTf did not lead to formation of a methylated diazenido product, instead producing Re(Me)(η^5-Cp)(BDI), and (2) reactions of Re(N=NSiMe_3)(η^5-Cp)(BDI) with MeOTf resulted only in formation of Re(Me)(η^5-Cp)(BDI) and unidentified side products. Collectively, these results confirm that the rhenium-group 9 dinitrogen complexes reported here are unique in their ability to methylate dinitrogen, likely due to a push-pull type interaction between the two metal centers, something that has not been previously demonstrated using other heterobimetallic transition metal complexes.

Concluding Remarks

We have reported rare examples of heterobimetallic dinitrogen complexes in the form of rhenium-group 9 species that adopt unusual, non-linear end-on/end-on geometries. More importantly, we were able to successfully methylate both the iridium and rhodium diazenido species, representing the first examples of N–C bond formation by heterobimetallic dinitrogen complexes. Our results also highlight the importance of the group 9 metal center, which is necessary for alkylation in this context, perhaps due to the group 9 metals' ability to aid in activating the dinitrogen fragment. Additionally, we were able to alter our initial reaction conditions to disfavor diazenido formation, with reactions run under argon instead leading to heterobimetallic bridging hydride complexes. Protonation of these metal hydrides led to rearrangements to form additional, alternative bridging hydride structures. Together, these results expand on the synthetic utility of the Na[Re(η^5-Cp)(BDI)] anion and demonstrate that it can be used for the functionalization of dinitrogen. The use of reducing metal centers in conjunction with cooperative transition metal partners in non-traditional coordination geometries is an emerging field, which will no doubt lead to more examples of dinitrogen activation and functionalization, and perhaps influence the design of future transition metal-mediated dinitrogen fixation catalysts.

Associated Content

Supporting Information

Experimental procedures, NMR data, FTIR data, crystallographic data, and computational details

Accession Codes

CCDC 2189790-21899797 contain the supplementary crystallographic data for this paper.

Author Information

Notes

The authors declare no competing financial interest.

Acknowledgements

This research was funded by the NSF (Grant No. CHE-1465188 and 1954612 to J.A. and R.G.B.). We thank Dr. Hasan Celik and UC Berkeley's NMR facility in the College of Chemistry (CoC-NMR) for spectroscopic assistance. Instruments in the CoC-NMR are supported in part by NIH S10OD024998. Dr.

Simon J. Teat is thanked for his assistance during crystallography experiments at the Advanced Light Source (ALS), and the ALS is supported by the Director, Office of Science, Office of Basic Energy Sciences, of the U.S. DOE under Contract No. DE-AC02-05CH11231. The UC Berkeley Molecular Graphics and Computation Facility is supported by the NIH (Grant No. S10OD023532) and Dr. David Small is thanked for assistance with computations. Dr. Jade I. Fostvedt and David Hales are thanked for helpful discussions. Prof. Simon Humphrey (University of Texas, Austin) is thanked for a generous donation of rhenium.

References

(1) Hidai, M.; Mizobe, Y. Recent Advances in the Chemistry of Dinitrogen Complexes. *Chem. Rev.* **1995**, *95* (4), 1115–1133.

(2) Nishibayashi, Y. Development of Catalytic Nitrogen Fixation Using Transition Metal-Dinitrogen Complexes under Mild Reaction Conditions. *Dalton Trans.* **2018**, *47*, 11290-11297.

(3) Nishibayashi, Y. *Transition Metal-Dinitrogen Complexes : Preparation and Reactivity*; Wiley-VCH, 2019.

(4) Chalkley, M. J.; Drover, M. W.; Peters, J. C. Catalytic N_2-to-NH_3(or -N_2H_4) Conversion by Well-Defined Molecular Coordination Complexes. *Chem. Rev.* **2020**, *120* (12), 5582–5636.

(5) Singh, D.; Buratto, W. R.; Torres, J. F.; Murray, L. J. Activation of Dinitrogen by Polynuclear Metal Complexes. *Chem. Rev.* **2020**, *120* (12), 5517–5581.

(6) Masero, F.; Perrin, M. A.; Dey, S.; Mougel, V. Dinitrogen Fixation: Rationalizing Strategies Utilizing Molecular Complexes. *Chem. - A Eur. J.* **2021**, *27* (12), 3892–3928.

(7) Lv, Z. J.; Wei, J.; Zhang, W. X.; Chen, P.; Deng, D.; Shi, Z. J.; Xi, Z. Direct Transformation of Dinitrogen: Synthesis of N-Containing Organic Compounds via N−C Bond Formation. *Natl. Sci. Rev.* **2020**, *7* (10), 1564–1583.

(8) Kim, S.; Loose, F.; Chirik, P. J. Beyond Ammonia: Nitrogen-Element Bond Forming Reactions with Coordinated Dinitrogen. *Chem. Rev.* **2020**, *120* (12), 5637–5681.

(9) Khoenkhoen, N.; De Bruin, B.; Reek, J. N. H.; Dzik, W. I. Reactivity of Dinitrogen Bound to Mid- and Late-Transition-Metal Centers. *Eur. J. Inorg. Chem.* **2015**, *2015* (4), 567–598.

(10) Burford, R. J.; Fryzuk, M. D. Examining the Relationship between Coordination Mode and Reactivity of Dinitrogen. *Nat. Rev. Chem.* **2017**, *1* (4), 1–13.

(11) Lindley, B. M.; Van Alten, R. S.; Finger, M.; Schendzielorz, F.; Würtele, C.; Miller, A. J. M.; Siewert, I.; Schneider, S. Mechanism of Chemical and Electrochemical N_2 Splitting by a Rhenium Pincer Complex. *J. Am. Chem. Soc.* **2018**, *140* (25), 7922–7935.

(12) Forrest, S. J. K.; Schluschaß, B.; Yuzik-Klimova, E. Y.; Schneider, S. Nitrogen Fixation via Splitting into Nitrido Complexes. *Chem. Rev.* **2021**, *121* (11), 6522–6587.

(13) Yamout, L. S.; Ataya, M.; Hasanayn, F.; Holland, P. L.; Miller, A. J. M.; Goldman, A. S. Understanding Terminal versus Bridging End-on N_2 Coordination in Transition Metal Complexes. *Cite This J. Am. Chem. Soc* **2021**, *143*, 9744–9757.

(14) Sickerman, N. S.; Peterson, S. M.; Ziller, J. W.; Borovik, A. S. Synthesis, Structure and Reactivity of $Fe^{II/III}$-NH_3 Complexes Bearing a Tripodal Sulfonamido Ligand. *Chem. Commun.* **2014**, *50* (19), 2515–2517.

(15) Creutz, S. E.; Peters, J. C. Exploring Secondary-Sphere Interactions in Fe-N_xH_y Complexes Relevant to N_2 Fixation. *Chem. Sci.* **2017**, *8* (3), 2321–2328.

(16) Bhattacharya, P.; Prokopchuk, D. E.; Mock, M. T. Exploring the Role of Pendant Amines in Transition Metal Complexes for the Reduction of N_2 to Hydrazine and Ammonia. *Coord. Chem. Rev.* **2017**, *334*, 67–83.

(17) Shanahan, J. P.; Szymczak, N. K. Hydrogen Bonding to a Dinitrogen Complex at Room Temperature: Impacts on N_2 Activation. *J. Am. Chem. Soc.* **2019**, *141* (21), 8550–8556.

(18) Geri, J. B.; Shanahan, J. P.; Szymczak, N. K. Testing the Push-Pull Hypothesis: Lewis Acid Augmented N2 Activation at Iron. *J. Am. Chem. Soc.* **2017**, *139* (16), 5952–5956.

(19) Coffinet, A.; Simonneau, A.; Specklin, D. Push–Pull Activation of N_2: Coordination of Lewis Acids to Dinitrogen Complexes. *Encycl. Inorg. Bioinorg. Chem.* **2020**, 1–25.

(20) The "push-pull" hypothesis describes a scenario in which a metal center donates (or "pushes") electron density towards the N_2 ligand through metal-ligand backbonding, while a Lewis acidic atom simultaneously interacts with the distal nitrogen atom to "pull" electron density away from the N_2 π^* orbitals, altogether leading to enhanced N_2 activation.[55]

(21) Pool, J. A.; Lobkovsky, E.; Chirik, P. J. Cyclopentadienyl Substituent Effects on Reductive Elimination Reactions in Group 4 Metallocenes: Kinetics, Mechanism, and Application to Dinitrogen Activation. *J. Am. Chem. Soc.* **2003**, *125* (8), 2241–2251.

(22) Fryzuk, M. D.; Johnson, S. A.; Patrick, B. O.; Albinati, A.; Mason, S. A.; Koetzle, T. F. New Mode of Coordination for the Dinitrogen Ligand: Formation, Bonding, and Reactivity of a Tantalum Complex with a Bridging N_2 Unit That Is Both Side-on and End-On. *J. Am. Chem. Soc.* **2001**, *123* (17), 3960–3973.

(23) Lohrey, T. D.; Bergman, R. G.; Arnold, J. Controlling Dinitrogen Functionalization at Rhenium through Alkali Metal Ion Pairing. *Dalt. Trans.* **2019**, *48* (48), 17936–17944.

(24) Chatt, J.; Dilworth, J. R.; Leigh, G. J.; Richards, R. L. Polynuclear Dinitrogen Complexes. *J. Chem. Soc. D Chem. Commun.* **1970**, No. 15, 955–956.

(25) Cradwick, P. D.; Chatt, J.; Crabtree, R. H.; Richards, R. L. Preparation and X-Ray Structure of a Trinuclear Dinitrogen-Bridged Complex, Trans-$[MoCl_4\{(N_2)ReCl(PMe_2Ph)_4\}_2]$. *J. Chem. Soc. Chem. Commun.* **1975**, *9*, 351–352.

(26) Schrock, R. R.; Kolodziej, R. M.; Liu, A. H.; Davis, W. M.; Vale, M. G. Preparation and Characterization of Two High Oxidation State Molybdenum Dinitrogen Complexes: $[MoCp^*Me_3]_2(\mu\text{-}N_2)$ and $[MoCp^*Me_3](\mu\text{-}N_2)[WCp'Me_3]$. *J. Am. Chem. Soc.* **1990**, *112* (11), 4338–4345.

(27) Mizobe, Y.; Yokobayashi, Y.; Oshita, H.; Takahashi, T.; Hidai, M. Preparation of Heterobimetallic Complexes with a Bridging Dinitrogen Ligand, $[WX(PMe_2Ph)_4(\mu\text{-}N_2)MCp_2Cl]$ (M = Ti, X = Cl; M = Zr, and Hf, X = I), and X-Ray Structure of $[WI(PMe_2Ph)_3(Py)(\mu\text{-}N_2)ZrCp_2Cl]$ (Py = Pyridine). *Organometallics* **1994**, *13* (10), 3764–3766.

(28) Odom, A. L.; Arnold, P. L.; Cummins, C. C. Heterodinuclear Uranium/Molybdenum Dinitrogen Complexes. *J. Am. Chem. Soc.* **1998**, *120*, 5836–5837.

(29) O'Donoghue, M. B.; Davis, W. M.; Schrock, R. R.; Reiff, W. M. Heterobimetallic Dinitrogen Complexes That Contain the $\{[N_3N]Mo\text{-}N{=}N\}$- Ligand. *Inorg. Chem.* **1999**, *38* (2), 243–252.

(30) Peters, J. C.; Cherry, J. P. F.; Thomas, J. C.; Baraldo, L.; Mindiola, D. J.; Davis, W. M.; Cummins, C. C. Redox-Catalyzed Binding of Dinitrogen by Molybdenum N-Tert- Hydrocarbylanilide Complexes: Implications for Dinitrogen Functionalization and Reductive Cleavage. *J. Am. Chem. Soc.* **1999**, *121* (43), 10053–10067.

(31) Ishino, H.; Nagano, T.; Kuwata, S.; Yokobayashi, Y.; Ishii, Y.; Hidai, M.; Mizobe, Y. Syntheses, Structures, and Reactivities of f Heterobimetallic Bridging Dinitrogen Complexes Containing Group 6 and Group 4 or 5 Transition Metals. *Organometallics* **2001**, *20* (1), 188–198.

(32) Zhang, Q. F.; Chim, J. L. C.; Lai, W.; Wong, W. T.; Leung, W. H. Bridged Dinitrogen Complexes of Iron and Chromium Porphyrins. *Inorg. Chem.* **2001**, *40* (11), 2470–2471.

(33) Ishino, H.; Takemoto, S.; Hirata, K.; Kanaizuka, Y.; Hidai, M.; Nabika, M.; Seki, Y.; Miyatake, T.; Suzuki, N. Olefin Polymerization Catalyzed by Titanium-Tungsten Heterobimetallic Dinitrogen Complexes. *Organometallics* **2004**, *23* (20), 4544–4546.

(34) Seymore, S. B.; Brown, S. N. Kinetic Effects in Heterometallic Dinitrogen Cleavage. *Inorg. Chem.* **2006**, *45* (23), 9540–9550.

(35) Cozzolino, A. F.; Silvia, J. S.; Lopez, N.; Cummins, C. C. Experimental and Computational Studies on the Formation of Cyanate from Early Metal Terminal Nitrido Ligands and Carbon Monoxide. *Dalt. Trans.* **2014**, *43* (12), 4639–4652.

(36) Specklin, D.; Coffinet, A.; Vendier, L.; Del Rosal, I.; Dinoi, C.; Simonneau, A. Synthesis, Characterization, and Comparative Theoretical Investigation of Dinitrogen-Bridged Group 6-Gold Heterobimetallic Complexes. *Inorg. Chem.* **2021**, *60* (8), 5545–5562.

(37) Ouellette, E. T.; Magdalenski, J. S.; Bergman, R. G.; Arnold, J. Applications of Low-Valent Transition Metalates: Development of a Reactive Noncarbonyl Rhenium(I) Anion. *Acc. Chem. Res.* **2022**, *55* (5).

(38) Chatt, J.; Dilworth, J. R.; Leigh, G. J. Dinitrogen Complexes of Rhenium(I) and Rhenium(II). *J. Chem. Soc. Dalt. Trans.* **1973**, *6*, 612–618.

(39) Chatt, J.; Heath, G. A.; Hooper, N. E.; Leigh, G. J. Direct Formation of Acylazo- and Aroylazo-Rhenium(III) Complexes from Rhenium(I) Dinitrogen Complexes. *J. Organomet. Chem.* **1973**, *57* (2), C67–C68.

(40) Klopsch, I.; Finger, M.; Würtele, C.; Milde, B.; Werz, D. B.; Schneider, S. Dinitrogen Splitting and Functionalization in the Coordination Sphere of Rhenium. *J. Am. Chem. Soc.* **2014**, *136* (19), 6881–6883.

(41) Schendzielorz, F.; Finger, M.; Abbenseth, J.; Würtele, C.; Krewald, V.; Schneider, S. Metal-Ligand Cooperative Synthesis of Benzonitrile by Electrochemical Reduction and Photolytic Splitting of Dinitrogen. *Angew. Chemie - Int. Ed.* **2019**, *58* (3), 830–834.

(42) Bruch, Q. J.; Connor, G. P.; Chen, C. H.; Holland, P. L.; Mayer, J. M.; Hasanayn, F.; Miller, A. J. M. Dinitrogen Reduction to Ammonium at Rhenium Utilizing Light and Proton-Coupled Electron Transfer. *J. Am. Chem. Soc.* **2019**, *141* (51), 20198–20208.

(43) Weber, J. E.; Hasanayn, F.; Fataftah, M.; Mercado, B. Q.; Crabtree, R. H.; Holland, P. L. Electronic and Spin-State Effects on Dinitrogen Splitting to Nitrides in a Rhenium Pincer System. *Inorg. Chem.* **2021**, *60* (9), 6115–6124.

(44) Na[Re(η5-Cp)(BDI)] easily reduces many TM metal salts, either by one or two electrons, to unproductively form reported Re(II) and Re(III) complexes: Re(η^5-Cp)(BDI)[50, 56] and Re(X)(η^5-Cp)(BDI) (X = Cl, Br, I, OTf).[54]

(45) Dilworth, J. R. Diazene, Diazenido, Isodiazene and Hydrazido Complexes. *Coord. Chem. Rev.* **2017**, *330*, 53–94.

(46) A search of the Cambridge Structural Database on 6-5-2022 revealed that reported end-on/end-on "M–N–N–M" fragments contained only near-linear M–N–N angles ranging from 153° to 180°, and reported end-on/side-on complexes contained M–N–N angles of 59° to 71° for the side-on interaction.

(47) Irikura, K. K. Experimental Vibrational Zero-Point Energies: Diatomic Molecules. *J. Phys. Chem. Ref. Data* **2007**, *36* (2), 389–397.

(48) Huber, K. P.; Herzberg, G. *Molecular Spectra and Molecular Structure*; Springer US, 1979.

(49) Ouellette, E. T.; Carpentier, A.; Joseph Brackbill, I.; Lohrey, T. D.; Douair, I.; Maron, L.; Bergman, R. G.; Arnold, J. σ or π? Bonding Interactions in a Series of Rhenium Metallotetrylenes. *Dalt. Trans.* **2021**, *50* (6), 2083–2092.

(50) Lohrey, T. D.; Maron, L.; Bergman, R. G.; Arnold, J. Heterotetrametallic Re-Zn-Zn-Re Complex Generated by an Anionic Rhenium(I) β-Diketiminate. *J. Am. Chem. Soc.* **2019**, *141* (2), 800–804.

(51) Brookhart, M.; Grant, B.; Volpe, A. F. $[(3,5\text{-}(CF_3)_2C_6H_3)_4B]^-$ $[H(OEt_2)_2]^+$: A Convenient Reagent for Generation and Stabilization of Cationic, Highly Electrophilic Organometallic Complexes. *Organometallics* **1992**, *11* (11), 3920–3922.

(52) Barrientos-Penna, C. F.; Einstein, F. W. B.; Jones, T.; Sutton, D. Bimetallic Aryldiazenido Complexes. Crystal and Molecular Structure of (η^5-C_5H_5)$(CO)_2$Mo(μ-$NNC_6H_4CH_3$)Re$(CO)_2$(η^5-C_5H_5) Possessing a μ-Aryldiazenido-N,N' Bridge. *Inorg. Chem.* **1983**, *22* (18), 2614–2617.

(53) Hillhouse, G. L.; Haymore, B. L.; Bistram, S. A.; Herrmann, W. A. New Bridging Mode for Organodiazo Ligands. Molecular Structure of (η^5-C_5H_5)$(CO)_2$W$(NNCH_3)$Cr$(CO)_5$. *Inorg. Chem.* **1983**, *22* (2), 314–318.

(54) Ouellette, E.; Amaro-Estrada, J. I.; Lussier, D.; Chakarawet, K.; Lohrey, T.; Maron, L.; Bergman, R.; Arnold, J. Spectroscopic, Magnetic, and Computational Investigations on a Series of Rhenium(III) Cyclopentadienide β-Diketiminate Halide and Pseudohalide Complexes. *Organometallics*, ahead of print, DOI: 10.1021/acs.organomet.1c00516.

(55) Hoffman, B. M.; Lukoyanov, D.; Yang, Z. Y.; Dean, D. R.; Seefeldt, L. C. Mechanism of Nitrogen Fixation by Nitrogenase: The Next Stage. *Chem. Rev.* **2014**, *114* (8), 4041–4062.

(56) Lohrey, T. D.; Rao, G.; Small, D. W.; Ouellette, E. T.; Bergman, R. G.; Britt, R. D.; Arnold, J. Electronic Structures of Rhenium(II) β-Diketiminates Probed by EPR Spectroscopy: Direct Comparison of an Acceptor-Free Complex to Its Dinitrogen, Isocyanide, and Carbon Monoxide Adducts. *J. Am. Chem. Soc.* **2020**, *142* (32), 13805–13813.

For Table of Contents Only